ACADEMIC PRESS

Available online at www.sciencedirect.com

SCIENCE DIRECT®

Journal of Sound and Vibration 260 (2003) 307–328

JOURNAL OF SOUND AND VIBRATION

www.elsevier.com/locate/jsvi

Semi-active damping control of suspension systems for specified operational response mode

Jeong-Hoon Kim, Chong-Won Lee*

Center for Noise and Vibration Control (NOVIC), Department of Mechanical Engineering, KAIST, Science Town, Daejeon 305-701, South Korea

Received 3 January 2002; accepted 30 April 2002

Abstract

A practical and effective semi-active on–off damping control law using semi-active actuators is developed for vibration attenuation of a natural, multi-degree-of-freedom suspension system, when its operational response mode is specified. It does not need the accurate system parameters and semi-active actuator dynamics. It reduces the total vibratory energy of the system including the work done by external disturbances and the maximum energy dissipation direction of the semi-active actuator is tuned to the operational response mode of the structure. The effectiveness of the control law using a single semi-active linear mount is illustrated with a three-degree-of-freedom excavator cabin suspension model.

1. Introduction

As the need for reduced noise and vibration increases, the suspension systems of machines and structures are becoming even more complex and more important than ever. Among others, the semi-active suspension system is known to be a good candidate for practical applications because it combines the advantages of passive and active suspension systems [1]. It provides far better performance than the passive suspension system, not requiring high-power actuators or supplies. Its performance is often not better, but it costs far less than the active suspension system, although the controller implementation remains almost identical.

Semi-active control laws, which are often developed by modifying active control laws, require an accurate and yet robust mathematical model of the structure and the control devices. Clipped-optimal control is perhaps one of the most commonly used semi-active control algorithms, due to

*Corresponding author. Tel.: +82-42-869-3016; fax: +82-42-869-8220.
E-mail address: cwlee@novic.kaist.ac.kr (C.-W. Lee).

0022-460X/03/$ - see front matter
PII: S0022-460X(02)00971-9

its robustness to change of the system parameters. On the other hand, semi-active control devices possess inherent non-linearity so that development of optimal control laws becomes challenging. As the suspension technology advances, many passive suspension systems have been replaced by semi-active suspension systems. The stringent performance requirement for semi-active suspension systems is the simple implementation, not the best isolation. Thus, numerous semi-active on–off control algorithms have been developed and adopted for semi-active control systems, which are robust to modelling uncertainties. The 'sky-hook' damper control algorithm has been commonly adopted for vehicle suspension systems and demonstrated its improved performance over passive systems when applied to a single-degree-of-freedom system [2]. Recently, a control algorithm based on Lyapunov's direct stability theory has been proposed for electro-rheological fluid dampers [3,4]. It reduces the responses by minimizing the cost function, the rate of change of a Lyapunov function, where the state weighting matrix is to be properly selected. The decentralized bang–bang controller [5] acts to minimize the total energy in the structure. The maximum energy dissipation controller [6] uses the total relative vibratory energy in the system as a Lyapunov function. In this paper, an efficient semi-active on–off damping control law for a multi-degree-of-freedom suspension system is developed from Lagrange's equations of motion, using the idea of Lyapunov's direct method. It minimizes the total vibratory energy of the structure, including the work done by external disturbances, whereas the dissipative energy of the semi-active control device is maximized for the specified vibrational response of the system. A numerical example is treated to demonstrate the application of the proposed control algorithm to a three-degree-of-freedom cabin suspension system with a single semi-active linear mount.

2. Lagrange's equations of motion

The equations of motion of a vibratory system can be derived from the Lagrangian L, expressed in terms of generalized co-ordinates as [7]

$$L = T - V, \tag{1}$$

where T and V represent the kinetic and potential energies of the system, respectively. The extended Lagrange's equation, including the dissipative energy term, can be stated, for an n-degree-of-freedom system, as

$$\frac{\mathrm{d}}{\mathrm{d}t}\left(\frac{\partial L}{\partial \dot{q}_k}\right) - \frac{\partial L}{\partial q_k} + \frac{\partial R}{\partial \dot{q}_k} = Q_k, \quad k = 1, 2, \ldots, n, \tag{2}$$

where q_k is the generalized co-ordinates, Q_k denotes the non-potential forces and R is the Rayleigh dissipation function.

3. Semi-active control system

Semi-active control system originates from a passive control system that has been subsequently modified to allow for adjustment of mechanical properties. The mechanical properties of the system may be adjusted based on feedback of the excitation and/or the measured response. The

control force in a semi-active control system normally acts to oppose the motion of the system, promoting the global stability of the structure. Semi-active control systems maintain the reliability of passive control systems and, yet, take the advantage of the adjustable parameter characteristics of active control systems. Among others, energy dissipation devices, which dissipate energy through various mechanisms such as shearing of viscous fluid, orificing of fluid, and sliding friction, have commonly been modified to behave in a semi-active manner [8]. Without loss of generality, a semi-active control force, F_i, may be modelled as a linear damper with controllable damping, i.e.,

$$F_i = v_i(t)\dot{r}_i(\mathbf{q}, \dot{\mathbf{q}}, \dot{\mathbf{y}}), \tag{3}$$

where $r_i(\mathbf{q}, \mathbf{y})$ is the relative position between two ends of the ith semi-active device, $\mathbf{q}$ and $\dot{\mathbf{q}}$ denote the n-dimensional vectors with components of generalized co-ordinates q_k and generalized velocities $\dot{q}_k$, respectively, $\mathbf{y}(t)$ and $\dot{\mathbf{y}}(t)$ are the d-dimensional external disturbance vectors with components of dispacements y_j and velocities $\dot{y}_j$, $j = 1$ to d, where d is the number of external disturbances, $v_i(t)$ is the variable damping coefficient with $0 \leqslant v_{i\,min} \leqslant v_i(t) \leqslant v_{i\,max}$, $i = 1$ to p, where p is the number of semi-active devices, $v_{i\,min}$ and $v_{i\,max}$ are the smallest and largest allowable values for v_i, respectively. For a semi- active vibration control system, Rayleigh's dissipation function R can be expressed as

$$R = R_v + R_c, \tag{4}$$

where

$$R_v = \frac{1}{2}\sum_{i=1}^{p}(v_i\dot{r}_i^2) \quad \text{and} \quad R_c = \frac{1}{2}\sum_{i=p+1}^{p+s}(c_i\dot{r}_i^2),$$

c_i and r_i, for $i = p+1$ to $p+s$, are the damping coefficient of a passive device and the relative position between two ends of the device, where s is the number of the passive devices. Here, R_v and R_c are the Rayleigh dissipation functions derived from the semi-active control forces and the original passive dissipative forces, respectively. We assume that the original system (2) is always stable.

4. Control strategy: maximizing energy dissipation rate

Let us introduce the *Hamiltonian function*, H, defined by

$$H = \sum_{k=1}^{n}\frac{\partial L}{\partial \dot{q}_k}\dot{q}_k - L. \tag{5}$$

For a natural system, the Hamiltonian reduces to the total energy of the system [7]

$$H = T + V = E. \tag{6}$$

Then, the rate of change in the total system energy is expressed as

$$\dot{H} = \dot{H}_q + \dot{H}_y, \tag{7}$$

where

$$\dot{H}_q = \sum_{k=1}^{n} \left(\frac{\mathrm{d}}{\mathrm{d}t} \left(\frac{\partial L}{\partial \dot{q}_k} \right) \dot{q}_k - \frac{\partial L}{\partial q_k} \dot{q}_k \right) \quad \text{and} \quad \dot{H}_y = - \sum_{j=1}^{d} \frac{\partial L}{\partial y_j} \dot{y}_j.$$

Here, $\dot{H}_q$ is the rate of change in the system energy and $\dot{H}_y$ is the energy inflow rate due to the external disturbances applied to the system. Because the kinetic energy of the system does not depend on y_j, $\partial L/\partial y_j = -\partial V/\partial y_j$. When there are dissipative forces derived from the Rayleigh dissipation function R in Eq. (4), we can obtain, using Lagrange's equation (2),

$$\dot{H}_q = \dot{H}_v + \dot{H}_c, \tag{8}$$

where

$$\dot{H}_v = - \sum_{i=1}^{p} v_i \dot{r}_i \left(\sum_{k=1}^{n} \frac{\dot{r}_i}{\partial \dot{q}_k} \dot{q}_k \right) \quad \text{and} \quad \dot{H}_c = - \sum_{i=p+1}^{p+s} c_i \dot{r}_i \left(\sum_{k=1}^{n} \frac{\dot{r}_i}{\partial \dot{q}_k} \dot{q}_k \right).$$

Here, $\dot{H}_c$ is the energy dissipation rate due to the original passive dampings in the system and is not directly controllable by changing the semi-active control forces. So, a semi-active control effort should be made such that the magnitude of $\dot{H}_v$, the energy dissipation rate due to the semi-active control forces, is maximized. The semi-active control strategy, proposed in this work, is based on a fundamental physical observation: if the total energy of a mechanical system is continuously dissipated, then the system, *linear or non-linear*, must eventually settle down to an equilibrium point. The mathematical extension of this observation is the basic philosophy of Lyapunov's theory [9]. The variable damping coefficients of the semi-active control devices should be set to be dissipative for interested generalized co-ordinates of the system and thus to make $\dot{H}_v$ negative. But, because of the semi-active nature of control forces restrictions and the presence of external disturbances, it is impractical to keep $\dot{H}_v$ always negative. However, it becomes feasible to keep $\dot{H}_v$ negative while the semi-active control is activated. For that purpose, the variable damping coefficient $v_i(t)$ may be determined as

$$\text{if } \dot{r}_i \left(\sum_{k=1}^{n} \rho_{ik} \frac{\partial \dot{r}_i}{\partial \dot{q}_k} \dot{q}_k \right) \geqslant 0, \quad \text{then } v_i = v_{i\,max}, \tag{9a}$$

$$\text{if } \dot{r}_i \left(\sum_{k=1}^{n} \rho_{ik} \frac{\partial \dot{r}_i}{\partial \dot{q}_k} \dot{q}_k \right) < 0, \quad \text{then } v_i = v_{i\,min}, \tag{9b}$$

where ρ_{ik} is the weighting factor imposed on the kth generalized co-ordinate associated with the ith semi-active device. For a single-degree-of-freedom system, the proposed control, Eq. (9), reduces to the well-known 'sky-hook' damper control. Typical applications to two-degree-of-freedom systems include the pitch–plane model of a vehicle and the quarter car suspension model of a vehicle. For the pitch–plane model, control algorithm (9) with $\rho_{i1} = \rho_{i2} = 1$ is equivalent to the sky-hook damper control applied to the ith semi-active actuator which is mounted in parallel to the ith suspension. On the other hand, for the quarter car suspension model, it is equivalent to placing a passive damper in parallel to the suspension element.

From Eq. (9), $\dot{H}_v$ becomes, since $p = p_u + p_l$,

$$\begin{aligned}\dot{H}_v &= -\sum_{k=1}^{n} \frac{\partial R_v}{\partial \dot{q}_k}\dot{q}_k \\ &= -\sum_{i=1}^{P_u} \frac{v_{i\,max}\ \|\dot{r}_i\|}{\left\|\sum_{k=1}^{n} \rho_{ik}(\partial \dot{r}_i/\partial \dot{q}_k)\dot{q}_k\right\|}\left(\sum_{k=1}^{n} \rho_{ik}\,\frac{\partial \dot{r}_i}{\partial \dot{q}_k}\dot{q}_k\right)\left(\sum_{k=1}^{n} \frac{\partial \dot{r}_i}{\partial \dot{q}_k}\dot{q}_k\right) - \sum_{i=P_u+1}^{P_u+P_l} v_{i\,min}\dot{r}_i\left(\sum_{k=1}^{n} \frac{\partial \dot{r}_i}{\partial \dot{q}_k}\dot{q}_k\right),\end{aligned} \tag{10}$$

where P_u and P_l are the numbers of the semi-active control devices in operation which satisfy conditions (9a) and (9b), respectively. For most of practical cases where we can assume that $v_{i\,min}$ is zero, Eq. (10) reduces to

$$\begin{aligned}\dot{H}_v &\approx -\sum_{i=1}^{p} \frac{v_i\|\dot{r}_i\|}{\left\|\sum_{k=1}^{n} \rho_{ik}(\partial \dot{r}_i/\partial \dot{q}_k)\dot{q}_k\right\|}\left(\sum_{k=1}^{n} \rho_{ik}\frac{\partial \dot{r}_i}{\partial \dot{q}_k}\dot{q}_k\right)\left(\sum_{k=1}^{n} \frac{\partial \dot{r}_i}{\partial \dot{q}_k}\dot{q}_k\right) = -\sum_{i=1}^{p} \alpha_i\left(\sum_{k=1}^{n}\sum_{l=1}^{n} \rho_{ik}\frac{\partial \dot{r}_i}{\partial \dot{q}_k}\,\frac{\partial \dot{r}_i}{\partial \dot{q}_l}\dot{q}_k\dot{q}_l\right). \\ &= -\sum_{i=l}^{p} \alpha_i\dot{\mathbf{q}}^{\mathrm{T}}D_i\dot{q}\left(\equiv \sum_{i=1}^{p} \dot{H}_{vi}\right) = -\dot{\mathbf{q}}^{\mathrm{T}}\left[\sum_{i=1}^{p} \alpha_i\mathbf{D}_i\right]\dot{\mathbf{q}} = -\dot{\mathbf{q}}^{\mathrm{T}}[\alpha_1\mathbf{D}_1 + \alpha_2\mathbf{D}_2 + \cdots + \alpha_p\mathbf{D}_p]\dot{\mathbf{q}},\end{aligned} \tag{11}$$

where $\alpha_i = v_i\|\dot{r}_i\|/\left\|\sum_{k=1}^{n} \rho_{ik}(\partial \dot{r}_i/\partial \dot{q}_k)\dot{q}_k\right\|$; $\mathbf{D}_i$ is an $n \times n$ real symmetric matrix with elements of $\rho_{ik}(\partial \dot{r}_i/\partial \dot{q}_k)(\partial \dot{r}_i/\partial \dot{q}_l)$; and $\dot{H}_{vi}(\dot{\mathbf{q}}) \equiv -\alpha_i\dot{\mathbf{q}}^{\mathrm{T}}\mathbf{D}_i\dot{\mathbf{q}}$ is the ith term of $\dot{H}_v$. Note that, by control action (9), $\dot{H}_v$ becomes a quadratic form of generalized co-ordinates only.

5. Determination of weighting factors

The semi-active control algorithm (9) necessitates proper assignment of the weighting factors ρ_{ik}.

5.1. The maximum principle

For a real symmetric matrix $\mathbf{A}$, the quadratic form $Q(\dot{\mathbf{q}}) = \dot{\mathbf{q}}^{\mathrm{T}}\mathbf{A}\dot{\mathbf{q}}$ produces a real number for every vector $\dot{\mathbf{q}}$ in $\Re^n$. Since $Q(\dot{\mathbf{q}})$ is a continuous function in $\Re^n$, it attains a maximum on the closed, bounded set of vectors $\|\dot{\mathbf{q}}\| = 1$. The quadratic form attains the maximum λ_1 at $\dot{\mathbf{q}} = \boldsymbol{\varphi}_1$, where λ_1 is the largest eigenvalue of matrix $\mathbf{A}$ and $\boldsymbol{\varphi}_1$ is the eigenvector corresponding to λ_1. Then for every unit vector $\dot{\mathbf{q}}$ orthorgonal to $\boldsymbol{\varphi}_1$, $Q(\dot{\mathbf{q}}) \leqslant Q(\boldsymbol{\varphi}_1)$. But, on the subset $\dot{\mathbf{q}} \cdot \boldsymbol{\varphi}_1 = 0$, $\|\dot{\mathbf{q}}\| = 1$, $Q(\dot{\mathbf{q}})$ again attains a maximum λ_2 at $\dot{\mathbf{q}} = \boldsymbol{\varphi}_2$ where λ_2 is the second eigenvalue of the matrix $\mathbf{A}$ and $\boldsymbol{\varphi}_2$ is the eigenvector corresponding to λ_2. Continuing in this way we can get a set of mutually orthorgonal unit vectors $\boldsymbol{\varphi}_k$ at which the local extremal value λ_k is attained on the subset $\|\dot{\mathbf{q}}\| = 1$. We can also easily find that $\boldsymbol{\varphi}_k$ is in fact the kth eigenvector of $\mathbf{A}$ and that the value λ_k is the corresponding eigenvalue, $\lambda_1 \geqslant \lambda_2 \geqslant \cdots \geqslant \lambda_n$ [10].

From simple calculation, it is easily derived that matrix $\mathbf{D}_i$, has only two non-zero eigenvalues irrespective of the matrix dimension, n, except when all weighting factors are identical. The

eigenvalues are obtained to be

$$\lambda_+^i = \frac{1}{2}\left(\sum_{k=1}^{n}\left(\frac{\partial \dot{r}_i}{\partial \dot{q}_k}\right)^2 \rho_{ik} + \sqrt{\sum_{k=1}^{n}\left(\frac{\partial \dot{r}_i}{\partial \dot{q}_k}\right)^2}\right) \geqslant 0, \tag{12}$$

$$\lambda_-^i = \frac{1}{2}\left(\sum_{k=1}^{n}\left(\frac{\partial \dot{r}_i}{\partial \dot{q}_k}\right)^2 \rho_{ik} - \sqrt{\sum_{k=1}^{n}\left(\frac{\partial \dot{r}_i}{\partial \dot{q}_k}\right)^2}\right) \leqslant 0 \tag{13}$$

and the kth component of eigenvector $\boldsymbol{\varphi}_+^i$ corresponding to λ_+^i can also be easily obtained as

$$\varphi_{+k}^i = \frac{\partial \dot{r}_i}{\partial \dot{q}_k}\left(1 + \rho_{ik}\sqrt{\sum_{l=1}^{n}\left(\frac{\partial \dot{r}_i}{\partial \dot{q}_l}\right)^2}\right) \Bigg/ \sqrt{\sum_{l=1}^{n}\left(\frac{\partial \dot{r}}{\partial \dot{q}_l}\right)^2\left(1 + \rho_{il}\sqrt{\sum_{l=1}^{n}\left(\frac{\partial \dot{r}_i}{\partial \dot{q}_l}\right)^2}\right)^2}, \tag{14}$$

where

$$\sum_{k=1}^{n}\left(\frac{\partial \dot{r}_i}{\partial \dot{q}_k}\rho_{ik}\right)^2 = 1 \tag{15}$$

and the superscript i denotes that the eigensolutions are calculated from the matrix $\mathbf{D}_i$. When all weighting factors are identical, leading to the sky-hook damper control, there exists only one non-zero, positive eigenvalue. This can be easily deduced from Eqs. (12) and (13). From the previous discussion, $\dot{H}_{vi}$ attains its maximum energy dissipation rate on $\boldsymbol{\varphi}_+^i$. The weighting factors should then be properly assigned such that the eigenvector $\boldsymbol{\varphi}_+^i$ corresponding to λ_+^i is aligned with the excessive vibrational motion of interest. In this case, because the eigenvalues λ_-^i is negative, the vibration motion or mode corresponding to $\boldsymbol{\varphi}_-^i$ is little damped. It has little effect on $\dot{H}_{vi}$ because of the semi-active nature of control forces restrictions. So, $\dot{H}_{vi}$ produces a sum of squares as [10]

$$\dot{H}_{vi} = -\alpha_i \dot{\mathbf{q}}^{\mathrm{T}}\mathbf{D}_i\dot{\mathbf{q}} = -\alpha_i(\lambda_+^i(\eta_+^i)^2 + \lambda_-^i(\eta_-^i)^2) = -\alpha_i\lambda_+^i(\eta_+^i)^2. \tag{16}$$

where $\eta_+^i = \dot{\mathbf{q}}^{\mathrm{T}} \cdot \boldsymbol{\varphi}_+^i$ and $\eta_-^i = \dot{\mathbf{q}}^{\mathrm{T}} \cdot \boldsymbol{\varphi}_-^i$. Then, $\dot{H}_v$ can be rewritten as

$$\dot{H}_v = -\sum_{i=1}^{p}\alpha_i\dot{\mathbf{q}}^{\mathrm{T}}\mathbf{D}_i\dot{\mathbf{q}} = -\sum_{i=1}^{p}\alpha_i\lambda_+^i(\eta_+^i)^2. \tag{17}$$

Contrary to $\dot{H}_v$, $\dot{H}_c$ explicitly contains both the generalized co-ordinates and the external disturbances. So, it can be divided into two terms with the co-ordinates and the external disturbances, respectively, that is,

$$\dot{H}_c = \dot{H}_{cq} + \dot{H}_{cy} \tag{18}$$

and $\dot{H}_{cq}$, in general, can be represented in the quadratic form of

$$\dot{H}_{cq} = -\dot{\mathbf{q}}^{\mathrm{T}}\mathbf{C}\dot{\mathbf{q}}, \tag{19}$$

where $\mathbf{C}$ is the passive system damping matrix with elements of $\partial \dot{r}_i/\partial \dot{q}_k$ and c_i. When the system is linear or can be linearized in the neighborhood of an equilibrium, the damping matrix becomes

constant. Algebraically, $\dot{H}_{cq}$ produces a sum of squares as

$$\dot{H}_{cq} = -\sum_{k=1}^{n} \lambda_k (\eta_k)^2, \tag{20}$$

where λ_k denote the kth eigenvalue of the matrix $\mathbf{C}$, $\eta_k = \dot{\mathbf{q}}^{\mathrm{T}} \cdot \boldsymbol{\varphi}_k$ and $\boldsymbol{\varphi}_k$ is the kth eigenvector of the matrix $\mathbf{C}$ corresponding to λ_k. Then, the dissipation rate of the system energy $\dot{H}_q$ can be rewritten as

$$\dot{H}_q = \dot{H}_{cq} + \dot{H}_{cy} + \dot{H}_v = -\sum_{k=1}^{n} \lambda_k (\eta_k)^2 - \sum_{i=1}^{p} \alpha_i \lambda_+^i (\eta_+^i)^2 + \dot{H}_{cy}. \tag{21}$$

It is useful to note that, because the matrix $\mathbf{D}_i$ in Eq. (11) is also a function of $\partial \dot{r}_i / \partial \dot{q}_k$, which is related to the location of the ith semi-active control device, we can adjust the eigenvectors of $\mathbf{D}_i$, by changing the location of the ith semi-active control device.

5.2. Target vector selection

For proper assignment of the weighting factors, the excessive dominant vibrational motion of interest, namely the target vector should be specified to be aligned with the eigenvector $\boldsymbol{\varphi}_+^i$ corresponding to λ_+^i. The specified vibrational motion of interest may vary depending on the vibrational chracteristics of the system related to the energy storage and dissipation elements, the excitation and operational conditions, and the user's subjective requirement on the performance. In practice, the forced vibrations of many systems are often dominated by the so-called operational deflection shape, which can be a single natural mode or a combination of many natural modes. When the target vector is chosen as the dominant operational deflection shape of the interested system, its general form becomes a combination of natural modes. On the other hands, the least damped mode, which often causes excessive vibration, may be selected as the target vector. For example, we can select the target vector such that

$$\hat{\boldsymbol{\varphi}}^i \equiv \boldsymbol{\varphi}_n, \tag{22}$$

where $\boldsymbol{\varphi}_n$ is the eigenvector corresponding to the least eigenvalue λ_n and $\hat{\boldsymbol{\varphi}}^i$ is the target vector imposed on the ith semi-active device. In case when the least damped mode, $\boldsymbol{\varphi}_n$, is to be aligned with all the eigenvectors $\boldsymbol{\varphi}_+^i$ for $i = 1$ to p, implying that all semi-active control devices are engaged with a single target vector, the dissipation rate of the system energy $\dot{H}_q$ can be rewritten, from Eq. (21), as

$$\dot{H}_q = -\sum_{k=1}^{n-1} \lambda_k (\eta_k)^2 - \left(\lambda_n + \sum_{i=1}^{p} \alpha_i \lambda_+^i \right) (\eta_n)^2 + \dot{H}_{cy}. \tag{23}$$

Note that the amount of energy dissipation is significantly increased along with the target vector $\boldsymbol{\varphi}_n$.

5.3. Optimization

Eqs. (12) and (13) suggest that, in order to make λ_+^i large and λ_-^i small, all the weighting factors should be positive. With such constraint, the actuator eigenvector $\boldsymbol{\varphi}_+^i$ may not become aligned to

the specified target vector. Thus we find the n-dimensional weighting vector $\boldsymbol{\rho}_i = \{\rho_{i1}\rho_{i2}\ldots\rho_{in}\}$ for the ith semi-active control device, which minimizes the cost function

$$f(\boldsymbol{\rho}_i) = 1 - \ell(\boldsymbol{\varphi}_+^i(\boldsymbol{\rho}_i),\ \hat{\boldsymbol{\varphi}}^i) \tag{24}$$

subject to the n inequality constraints, from Eq. (15),

$$0 \leqslant \rho_{ik} \leqslant \frac{1}{|\partial \dot{r}_i/\partial \dot{q}_k|}; \quad k = 1 \text{ to } n, \tag{25}$$

where $0 \leqslant \ell(\mathbf{a},\mathbf{b}) = |\mathbf{a}^{\mathrm{T}}\mathbf{b}|/\|a\|\|b\| \leqslant 1$ is a measure of alignment between two vectors $\mathbf{a}$ and $\mathbf{b}$. Note that, when two vectors $\mathbf{a}$ and $\mathbf{b}$ are in line, $\ell(\mathbf{a},\mathbf{b}) = 1$, whereas $\ell(\mathbf{a},\mathbf{b}) = 0$ for $\mathbf{a} \perp \mathbf{b}$.

6. Illustrative example

As an example, vibration control of a three-degree-of-freedom excavator cabin suspension system is considered. Fig. 1 shows the dynamic model of the excavator cabin with a semi-active linear mount in the suspension, accounting for the bounce, pitch and roll motions of the cabin. For simplicity, it is assumed that the principal moment of inertia axes of the cabin coincide with the Cartesian co-ordinates as shown in Fig. 1. The Lagrangian L and Rayleigh's dissipation function R can be expressed as

$$\begin{aligned} L = T - V = {} & \tfrac{1}{2}(m\dot{z}^2 + I_{xx}\dot{\theta}_x^2 + I_{yy}\dot{\theta}_y^2) \\ & - \frac{1}{2}\begin{pmatrix} k_1(z + l_2\sin\theta_y - w_2\sin\theta_x - y_1)^2 + k_2(z - l_1\sin\theta_y - w_2\sin\theta_x - y_2)^2 \\ +k_3(z - l_1\sin\theta_y + w_1\sin\theta_x - y_3)^2 + k_4(z + l_2\sin\theta_y + w_1\sin\theta_x - y_4)^2 \end{pmatrix}, \end{aligned} \tag{26}$$

$$\begin{aligned} R = {} & R_c + R_v \\ = {} & \frac{1}{2}\begin{pmatrix} c_1(\dot{z} + l_2\cos\theta_y\dot{\theta}_y - w_2\cos\theta_x\dot{\theta}_x - \dot{y}_1)^2 + c_2(\dot{z} - l_1\cos\theta_y\dot{\theta}_y - w_2\cos\theta_x\dot{\theta}_x - \dot{y}_2)^2 \\ +c_3(\dot{z} - l_1\cos\theta_y\dot{\theta}_y + w_1\cos\theta_x\dot{\theta}_x - \dot{y}_3)^2 + c_4(\dot{z} + l_2\cos\theta_y\dot{\theta}_y + w_1\cos\theta_x\dot{\theta}_x - \dot{y}_4)^2 \end{pmatrix} \\ & + \tfrac{1}{2}v(\dot{z} + l_2\cos\theta_y\dot{\theta}_y - w_2\cos\theta_x\dot{\theta}_x - \dot{y}_1)^2, \end{aligned} \tag{27}$$

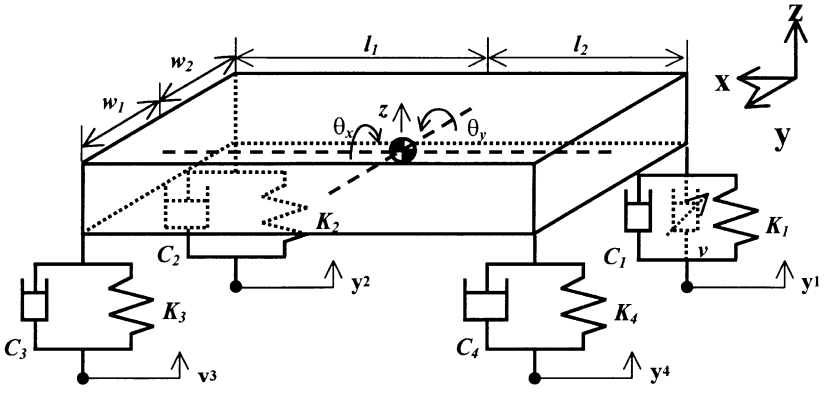

Fig. 1. Dynamic model of three-degree-of-freedom cabin suspension system.

where the semi-active mount is assumed to be placed at point 1 as shown in Fig. 1. The equations of motion are obtained as

$$\begin{aligned} m\ddot{z} &+ c_1(\dot{z} + l_2\cos\theta_y\dot{\theta}_y - w_2\cos\theta_x\dot{\theta}_x - \dot{y}_1) \\ &+ c_2(\dot{z} - l_1\cos\theta_y\dot{\theta}_y - w_2\cos\theta_x\dot{\theta}_x - \dot{y}_2) \\ &+ c_3(\dot{z} - l_1\cos\theta_y\dot{\theta}_y + w_1\cos\theta_x\dot{\theta}_x - \dot{y}_3) \\ &+ c_4(\dot{z} + l_2\cos\theta_y\dot{\theta}_y + w_1\cos\theta_x\dot{\theta}_x - \dot{y}_4) \\ &+ k_1(z + l_2\sin\theta_y - w_2\sin\theta_x - y_1) \\ &+ k_2(z - l_1\sin\theta_y - w_2\sin\theta_x - y_2) \\ &+ k_3(z - l_1\sin\theta_y + w_1\sin\theta_x - y_3) \\ &+ k_4(z + l_2\sin\theta_y + w_1\sin\theta_x - y_4) \\ &+ v(\dot{z} + l_2\cos\theta_y\dot{\theta}_y - w_2\cos\theta_x\dot{\theta}_x - \dot{y}_1) = 0, \end{aligned} \tag{28a}$$

$$\begin{aligned} I_{yy}\ddot{\theta}_y &+ c_1l_2\cos\theta_y(\dot{z} + l_2\cos\theta_y\dot{\theta}_y - w_2\cos\theta_x\dot{\theta}_x - \dot{y}_1) \\ &- c_2l_1\cos\theta_y(\dot{z} - l_1\cos\theta_y\dot{\theta}_y - w_2\cos\theta_x\dot{\theta}_x - \dot{y}_2) \\ &- c_3l_1\cos\theta_y(\dot{z} - l_1\cos\theta_y\dot{\theta}_y + w_1\cos\theta_x\dot{\theta}_x - \dot{y}_3) \\ &+ c_4l_2\cos\theta_y(\dot{z} + l_2\cos\theta_y\dot{\theta}_y + w_1\cos\theta_x\dot{\theta}_x - \dot{y}_4) \\ &+ k_1l_2\cos\theta_y(z + l_2\sin\theta_y - w_2\sin\theta_x - y_1) \\ &- k_2l_1\cos\theta_y(z - l_1\sin\theta_y - w_2\sin\theta_x - y_2) \\ &- k_3l_1\cos\theta_y(z - l_1\sin\theta_y + w_1\sin\theta_x - y_3) \\ &+ k_4l_2\cos\theta_y(z + l_2\sin\theta_y + w_1\sin\theta_x - y_4) \\ &+ vl_2\cos\theta_y(\dot{z} + l_2\cos\theta_y\dot{\theta}_y - w_2\cos\theta_x\dot{\theta}_x - \dot{y}_1) = 0, \end{aligned} \tag{28b}$$

$$\begin{aligned} I_{xx}\ddot{\theta}_x &- c_1w_2\cos\theta_x(\dot{z} + l_2\cos\theta_y\dot{\theta}_y - w_2\cos\theta_x\dot{\theta}_x - \dot{y}_1) \\ &- c_2w_2\cos\theta_x(\dot{z} - l_1\cos\theta_y\dot{\theta}_y - w_2\cos\theta_x\dot{\theta}_x - \dot{y}_2) \\ &+ c_3w_1\cos\theta_x(\dot{z} - l_1\cos\theta_y\dot{\theta}_y + w_1\cos\theta_x\dot{\theta}_x - \dot{y}_3) \\ &+ c_4w_1\cos\theta_x(\dot{z} + l_2\cos\theta_y\dot{\theta}_y + w_1\cos\theta_x\dot{\theta}_x - \dot{y}_4) \\ &- k_1w_2\cos\theta_x(z + l_2\sin\theta_y - w_2\sin\theta_x - y_1) \\ &- k_2w_2\cos\theta_x(z - l_1\sin\theta_y - w_2\sin\theta_x - y_2) \\ &+ k_3w_1\cos\theta_x(z - l_1\sin\theta_y + w_1\sin\theta_x - y_3) \\ &+ k_4w_1\cos\theta_x(z + l_2\sin\theta_y + w_1\sin\theta_x - y_4) \\ &- vw_2\cos\theta_x(\dot{z} + l_2\cos\theta_y\dot{\theta}_y - w_2\cos\theta_x\dot{\theta}_x - \dot{y}_1) = 0, \end{aligned} \tag{28c}$$

where z, θ_y and θ_x are the linear displacement and rotation angles of the cabin mass center along the z-, y- and x-axis; $\dot{y}_j$ and y_j, $j = 1, 2, 3, 4$, are the linear velocities and displacements at point j along the z-axis, acting as external distubances to the cabin. The system parameters and damping coefficient of the semi-active mount are listed in Table 1. The dissipation rate of the system energy

Table 1
System parameters

Symbol	Content	Value
m	Mass	602 kg
I_{xx}	Moment of inertia w.r.t. the x-axis	244.6 kgm^2
I_{yy}	Moment of inertia w.r.t. the y-axis	258.9 kgm^2
l_1	Length from mass center to mount 2 or 3 along the x-axis	961 mm
l_2	Length from mass center to mount 1 or 4 along the x-axis	931 mm
w_1	Length from mass center to mount 3 or 4 along the y-axis	480 mm
w_2	Length from mass center to mount 1 or 2 along the y-axis	480 mm
c_i	Damping coefficient of ith mount	30 N s/m
k_i	Stiffness coefficient of ith mount	20 kN/m
v_{max}	Maximum damping coefficient of semi-active mount	300 N s/m
v_{min}	Minimum damping coefficient of semi-active mount	0 N s/m

Table 1

$\dot{H}_q$ becomes

$$\begin{aligned}\dot{H}_q &= \dot{H}_c + \dot{H}_v \\ &= -c_1(\dot{z} + l_2\cos\theta_y\dot{\theta}_y - w_2\cos\theta_x\dot{\theta}_x - \dot{y}_1)(\dot{z} + l_2\cos\theta_y\dot{\theta}_y - w_2\cos\theta_x\dot{\theta}_x) \\ &\quad - c_2(\dot{z} - l_1\cos\theta_y\dot{\theta}_y - w_2\cos\theta_x\dot{\theta}_x - \dot{y}_2)(\dot{z} - l_1\cos\theta_y\dot{\theta}_y - w_2\cos\theta_x\dot{\theta}_x) \\ &\quad - c_3(\dot{z} - l_1\cos\theta_y\dot{\theta}_y + w_1\cos\theta_x\dot{\theta}_x - \dot{y}_3)(\dot{z} - l_1\cos\theta_y\dot{\theta}_y + w_1\cos\theta_x\dot{\theta}_x) \\ &\quad - c_4(\dot{z} + l_2\cos\theta_y\dot{\theta}_y + w_1\cos\theta_x\dot{\theta}_x - \dot{y}_4)(\dot{z} + l_2\cos\theta_y\dot{\theta}_y + w_1\cos\theta_x\dot{\theta}_x) \\ &\quad - v(\dot{z} + l_2\cos\theta_y\dot{\theta}_y - w_2\cos\theta_x\dot{\theta}_x - \dot{y}_1)(\dot{z} + l_2\cos\theta_y\dot{\theta}_y - w_2\cos\theta_x\dot{\theta}_x). \end{aligned} \tag{29}$$

Note here that the passive mounts with dampings of c_i, $i = 1, 2, 3, 4$, do not always extract energy from the system, because $\dot{H}_c$ becomes indefinite in the presence of external disturbances $\dot{y}_j$, $j = 1, 2, 3, 4$. Assuming the small motion, $\dot{H}_{cq}$ can be approximated as a quadratic form of

$$\dot{H}_{cq} = -\dot{\mathbf{q}}^{\mathrm{T}}\mathbf{C}\dot{\mathbf{q}}, \tag{30}$$

where

$$C = \begin{bmatrix} c_1 + c_2 + c_3 + c_4 & l_2(c_1 + c_4) - l_1(c_2 + c_3) & w_1(c_3 + c_4) - w_2(c_1 + c_2) \\ l_2(c_1 + c_4) - l_1(c_2 + c_3) & l_2^2(c_1 + c_4) + l_1^2(c_2 + c_3) & w_2(l_1c_2 - l_2c_1) - w_1(l_1c_3 - l_2c_4) \\ w_1(c_3 + c_4) - w_2(c_1 + c_2) & w_2(l_1c_2 - l_2c_1) - w_1(l_1c_3 - l_2c_4) & w_2^2(c_1 + c_2) + w_1^2(c_3 + c_4) \end{bmatrix}$$

and $\dot{\mathbf{q}}^{\mathrm{T}} = \{z\ \ \dot{\theta}_y\ \ \dot{\theta}_x\}$. The three eigenvalues and the corresponding normalized eigenvectors of the matrix $\mathbf{C}$ are obtained as $\lambda_1 = 120.3$, $\boldsymbol{\varphi}_1 = \{0.14\ -0.99\ 0\}^{\mathrm{T}}$; $\lambda_2 = 107.2$ $\boldsymbol{\varphi}_2 = \{-0.14\ -0.99\ 0)^{\mathrm{T}}$; and $\lambda_3 = 27.7$, $\boldsymbol{\varphi}_3 = \{0\,0\,1)$, respectively. Note that the roll motion is decoupled from the other two eigenvectors and least damped, when the four supporting passive mounts are identical. The proposed control law gives the variable damping of the semi-active mount as

$$\begin{gathered} \textit{if } (\dot{z} + l_2\cos\theta_y\dot{\theta}_y - w_2\cos\theta_x\dot{\theta}_x - \dot{y}_1)(\rho_1\dot{z} + \rho_2 l_2\cos\theta_y\dot{\theta}_y - \rho_3 w_2\cos\theta_x\dot{\theta}_x) \geqslant 0, \quad v = v_{max} \\ \textit{else, } v = v_{min} \end{gathered} \tag{31}$$

By the control action, $\dot{H}_{dv}$ can be approximated as a quadratic form given by

$$\begin{aligned}\dot{H}_{dv} &= -v(\rho_1\dot{z} + \rho_2 l_2 \cos\theta_y\dot{\theta}_y - \rho_3 w_2 \cos\theta_x\dot{\theta}_x)(\dot{z} + l_2\cos\theta_y\dot{\theta}_y - w_2\cos\theta_x\dot{\theta}_x)\\ &\cong -\alpha\dot{\mathbf{q}}^{\mathrm{T}}\mathbf{D}\dot{\mathbf{q}},\end{aligned} \tag{32}$$

where

$$\alpha = \frac{v\|\dot{z} + l_2\dot{\theta}_y - w_2\dot{\theta}_x - \dot{y}_1\|}{\|\rho_1\dot{z} + \rho_2 l_2\dot{\theta}_y - \rho_3 w_2\dot{\theta}_x\|},$$

$$\mathbf{D} = \begin{bmatrix} \rho_1 & \dfrac{\rho_1+\rho_2}{2}l_2 & -\dfrac{\rho_1+\rho_3}{2}w_2 \\ \dfrac{\rho_1+\rho_2}{2}l_2 & \rho_2 l_2^2 & -\dfrac{\rho_2+\rho_3}{2}l_2 w_2 \\ -\dfrac{\rho_1+\rho_3}{2}w_2 & -\dfrac{\rho_2+\rho_3}{2}l_2 w_2 & \rho_3 w_2^2 \end{bmatrix}.$$

The shaded area in Fig. 2(a) shows the feasible region of the eigenvector, $\boldsymbol{\varphi}_+$, associated with the above matrix $\mathbf{D}$, that is defined for the system with a single semi-active device mounted at point 1 and satisfies constraint (25). Note that the north hemisphere of unit radius corresponds to the allowable region of $\boldsymbol{\varphi}_+$ for the weighting vector subject to no constraint.

For the sky-hook damper control, where $\boldsymbol{\rho}_s^{\mathrm{T}} = \{\rho_{s1}\ \rho_{s2}\ \rho_{s3}\} = \{0.69\ 0.69\ 0.69\}$, we obtain $\lambda_{s+} = 1.45$ and $\boldsymbol{\varphi}_{s+} = \{-0.69\ -0.64\ 0.33\}^{\mathrm{T}}$ (marked 'S' in Fig. 2). Note that $\boldsymbol{\varphi}_{s+}$ can be expressed as a linear combination of the three eigenvectors, $\boldsymbol{\varphi}_1$, $\boldsymbol{\varphi}_2$ and $\boldsymbol{\varphi}_3$, of the matrix $\mathbf{C}$, i.e.,

$$\boldsymbol{\varphi}_{s+} = (0.59)\boldsymbol{\varphi}_1 + (0.73)\boldsymbol{\varphi}_2 + (0.33)\boldsymbol{\varphi}_3. \tag{33}$$

This action may not be desirable because the least damped roll motion is least attenuated. Similarly as before, the measure of alignment ℓ_s of a weighting vector $\boldsymbol{\rho}^T = \{\rho_1\ \rho_2\ \rho_3\}$ to $\boldsymbol{\rho}_s^{\mathrm{T}} = \{0.69\ \ 0.69\ \ 0.69\}$, which is associated with the sky-hook damper control, can be defined as

$$0 \leqslant \ell_s = \ell(\boldsymbol{\rho}, \boldsymbol{\rho}_s) \leqslant 1. \tag{34}$$

The value of ℓ_s indicates the degree of resemblance in performance of the proposed on–off damping control system designed with the weighting vector $\boldsymbol{\rho}$, compared to the sky-hook damper control system. The performance of the on–off damping control system designed with ℓ_s close to 1 will not significantly differ from the sky-hook damper control system. Fig. 2(b) shows the contour map of ℓ_s when the target vector $\hat{\boldsymbol{\varphi}}$ is specified within the feasible region. It will be demonstrated later that, if $\boldsymbol{\rho}$ is chosen such that the corresponding value of ℓ_s is close to 1, there are not much benefits in performance of the proposed on–off damping control against the sky-hook damper control. In other words, when the target vector is specified such that the corresponding value of ℓ_s is far less than 1 (for example, $\ell_s = 0.58$ for point P_A), the proposed on–off damping control scheme becomes far more beneficial in performance than the sky-hook damper control.

Now, let us choose the target vector as (marked 'T_A' in Fig. 2)

$$\hat{\boldsymbol{\varphi}}_A \equiv \boldsymbol{\varphi}_3 = \{\,0 \quad 0 \quad 1\,\}^{\mathrm{T}} \tag{35}$$

so that the semi-active mount can extract energy mostly from the least damped roll motion. Then, optimization (24) gives: $\boldsymbol{\rho}_{\mathrm{A}}^{\mathrm{T}} = \{\,\rho_1 \quad \rho_2 \quad \rho_3\,\} = \{\,0 \quad 0 \quad 2.08\,\}$, $\boldsymbol{\varphi}_A\ \lambda_{A+} = 0.96$ and $\boldsymbol{\varphi}_{A+} = \{-0.42\ -0.39\ 0.82\}$, $\boldsymbol{\varphi}_A$ (marked 'P_A' in Fig. 2). Note that $\boldsymbol{\varphi}_{A+}$ is not perfectly aligned to $\boldsymbol{\varphi}_A \equiv \boldsymbol{\varphi}_3$, giving

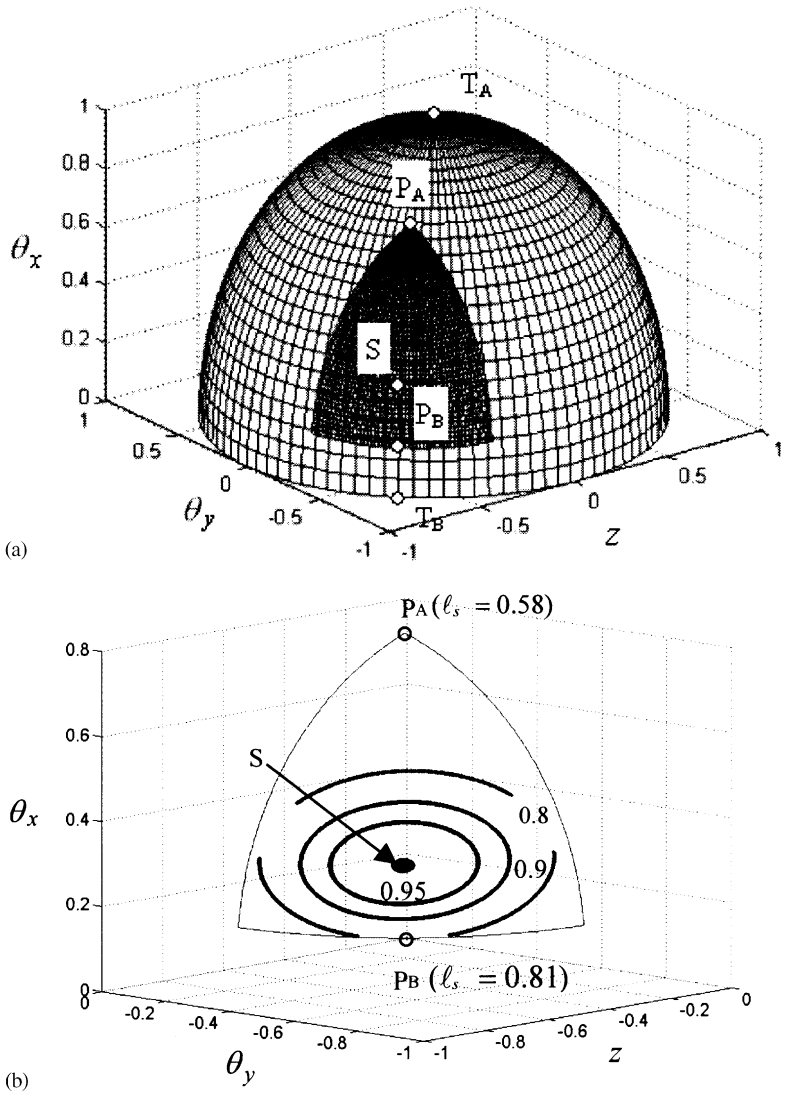

Fig. 2. Feasible region of eigenvector, $\boldsymbol{\varphi}_+$: (a) feasible region; (b) contour map of ℓ_s.

the measure of alignment of 0.67. The inevitable discrepancy is due to the inadequate location of the semi-active device and the inequality constraints imposed on the weighting factors, Eq. (25). Again, $\boldsymbol{\varphi}_{A+}$ can be expressed as

$$\boldsymbol{\varphi}_{A+} = (0.36)\boldsymbol{\varphi}_1 + (0.45)\boldsymbol{\varphi}_2 + (0.82)\boldsymbol{\varphi}_3 \approx \boldsymbol{\varphi}_3. \tag{36}$$

Note that the least-damped roll mode is most attenuated. When the system is subject to disturbances, the response vector can be decomposed as

$$\mathbf{q} = u_1\boldsymbol{\varphi}_1 + u_2\boldsymbol{\varphi}_2 + u_3\boldsymbol{\varphi}_3, \tag{37}$$

where $u_i = \mathbf{q}^{\mathrm{T}} \cdot \boldsymbol{\varphi}_i$ is the component of $\mathbf{q}$ along $\boldsymbol{\varphi}_i$.

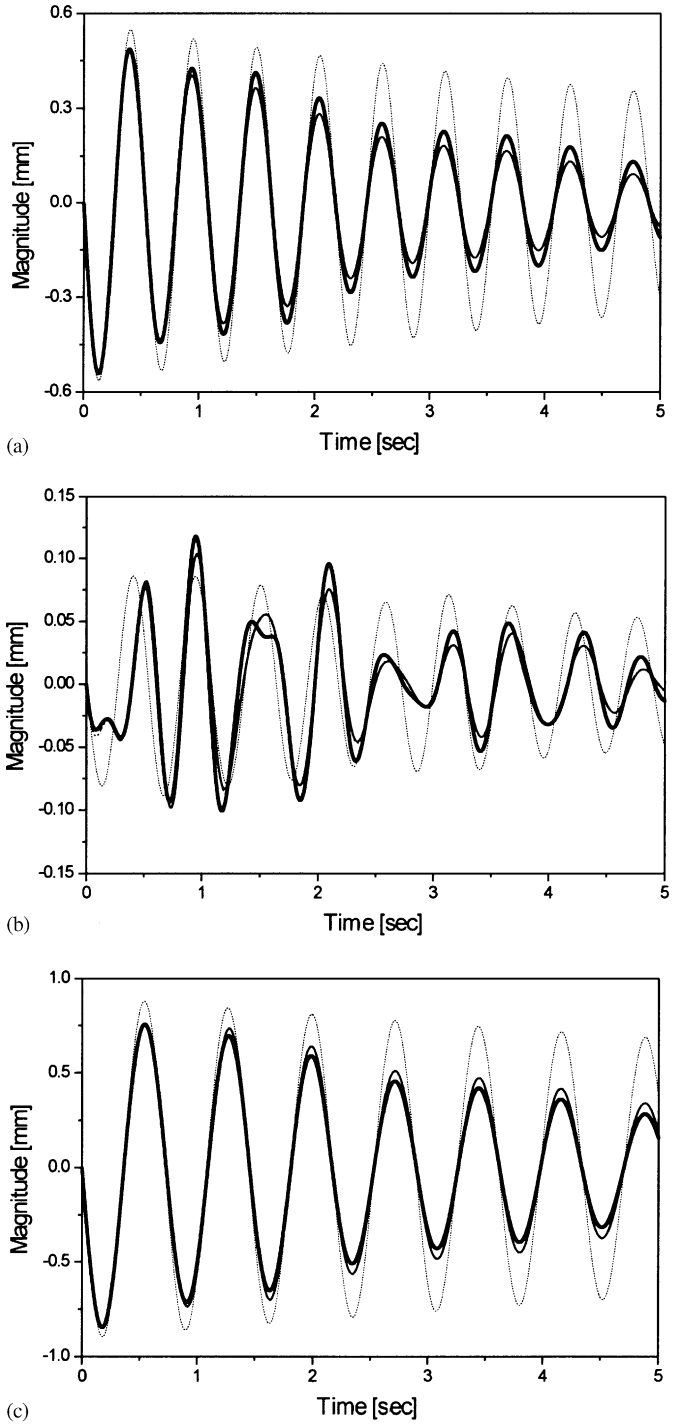

Fig. 3. Responses of the suspension system to the impulse disturbances at points 1 and 2. (a) Bounce-dominant motion, $u_1(t)$, (b) pitch-dominant motion, $u_2(t)$, and (c) roll motion, $u_3(t)$: ……, original system; ——, passive control system; ——, sky-hook control system; ——, proposed on–off control system ($\rho_1 = \rho_2 = 0, \rho_3 = 2.08$).

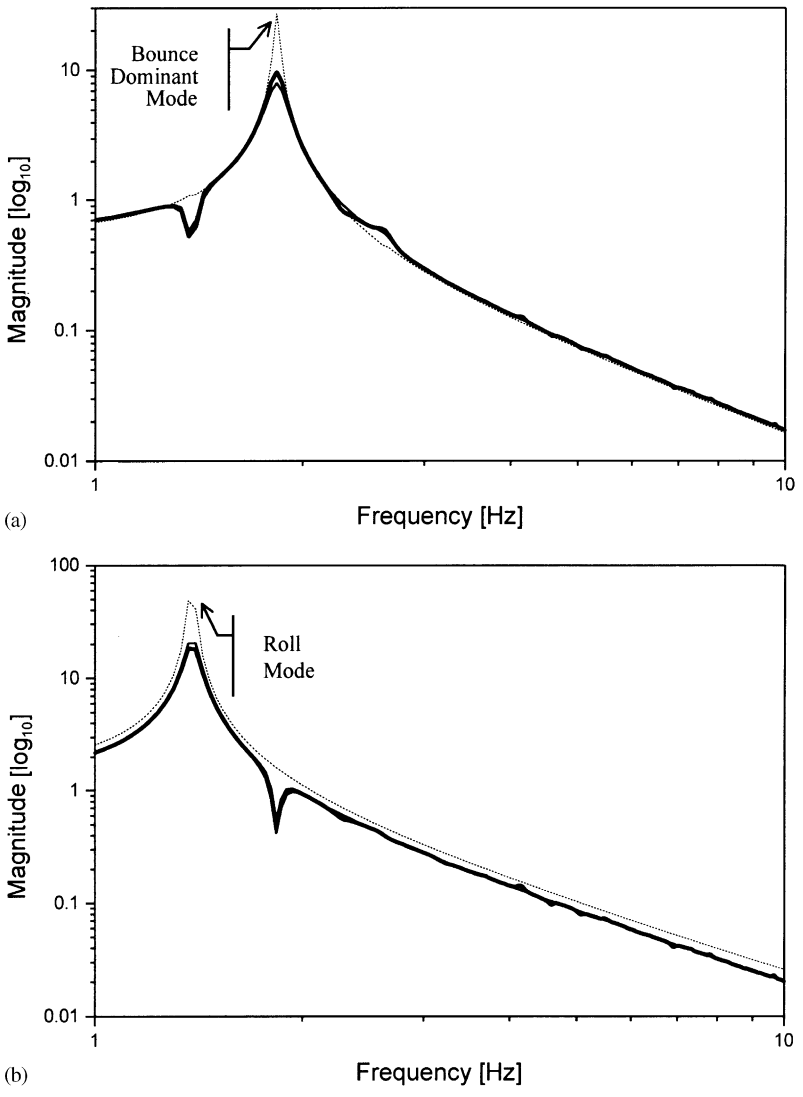

Fig. 4. Frequency response functions. (a) Bounce-dominant motion and (b) roll motion to the impulse disturbances at points 1 and 2: ……, original system; ——, passive control system; ——, sky-hook control system ($\rho_1 = \rho_2 = \rho_3 = 0.69$); ——, proposed on–off control system.

In the simulations, we compared the performances of the following four cases:

1. original system,
2. passive damping control system which merely adds a passive mount of v_{max} at point 1,
3. sky-hook damper control system which is equivalent to $\rho_1 = \rho_2 = \rho_3 = 0.69$, (marked 'S' in Fig. 2); and
4. proposed on–off damping control system with weighting factors of $\rho_1 = 0$, $\rho_2 = 0$ and $\rho_3 = 2.08$ (marked 'P_A' in Fig. 2).

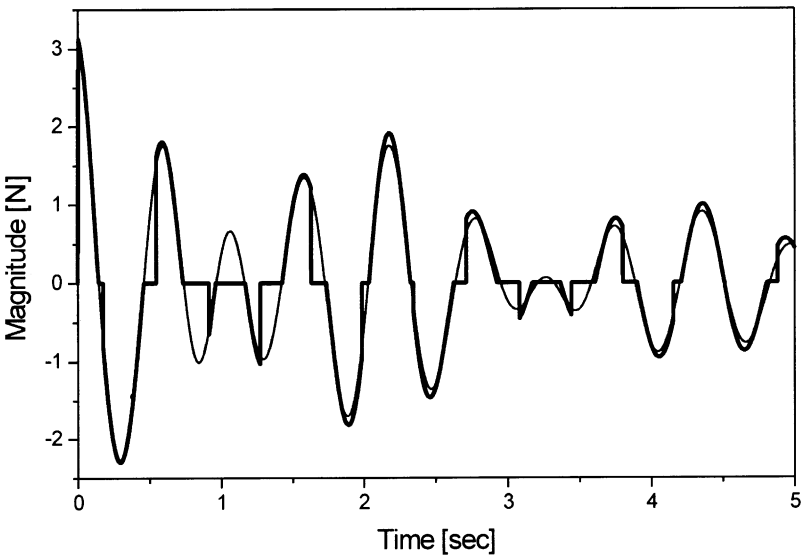

Fig. 5. Control forces to the impulse disturbances at points 1 and 2: ——, sky-hook control system ($\rho_1 = \rho_2 = \rho_3 = 0.69$); ——, proposed on–off control system.

The systems are equally subject to the two kinds of inputs, impulse disturbances at points 1 and 2, and 1 and 4, respectively, given by

$$y_1 = y_2 = (0.1)\delta(t); \text{ roll and bounce dominant input,} \tag{38a}$$

and

$$y_1 = y_4 = (0.1)\delta(t); \text{ pitch and bounce dominant input,} \tag{38b}$$

where $\delta(t)$ is the Dirac delta function. We first obtain the results for the above four cases under the roll and bounce dominant input (38a). Fig. 3 shows the impulse responses associated with the three components u_i, $i = 1, 2, 3$, of $\mathbf{q}$. Note that the roll motion, u_3, is much larger than the bounce and pitch dominant motions, u_1 and u_2, respectively, because of the nature of the input and the damping characteristics of the original system. Responses of the passive and the sky-hook damper control systems are not distinguable because, except at $t = 0$, there are no external disturbances. The proposed on–off control system gives smaller (larger) values of u_3 (u_1 and u_2) than the passive and the sky-hook damper control systems. Fig. 4 shows the Fourier transforms of the impulse responses of u_1 and u_3 normalized by the intensity of the impulse input. The results shown in the frequency domain also confirm that the proposed on–off control system shows better attenuation for the roll motion than the passive and the sky-hook damper control systems. Fig. 5 compares the corresponding control forces of the sky-hook damper control and the proposed on–off control, indicating that the magnitudes of the two control forces are similar. Note that the variable damping coefficient of the semi-active device mounted at point 1 always becomes v_{max}, the maximum damping coefficient. Because, except for at $t = 0$, there are no external disturbances, it virtually acts as a passive mount.

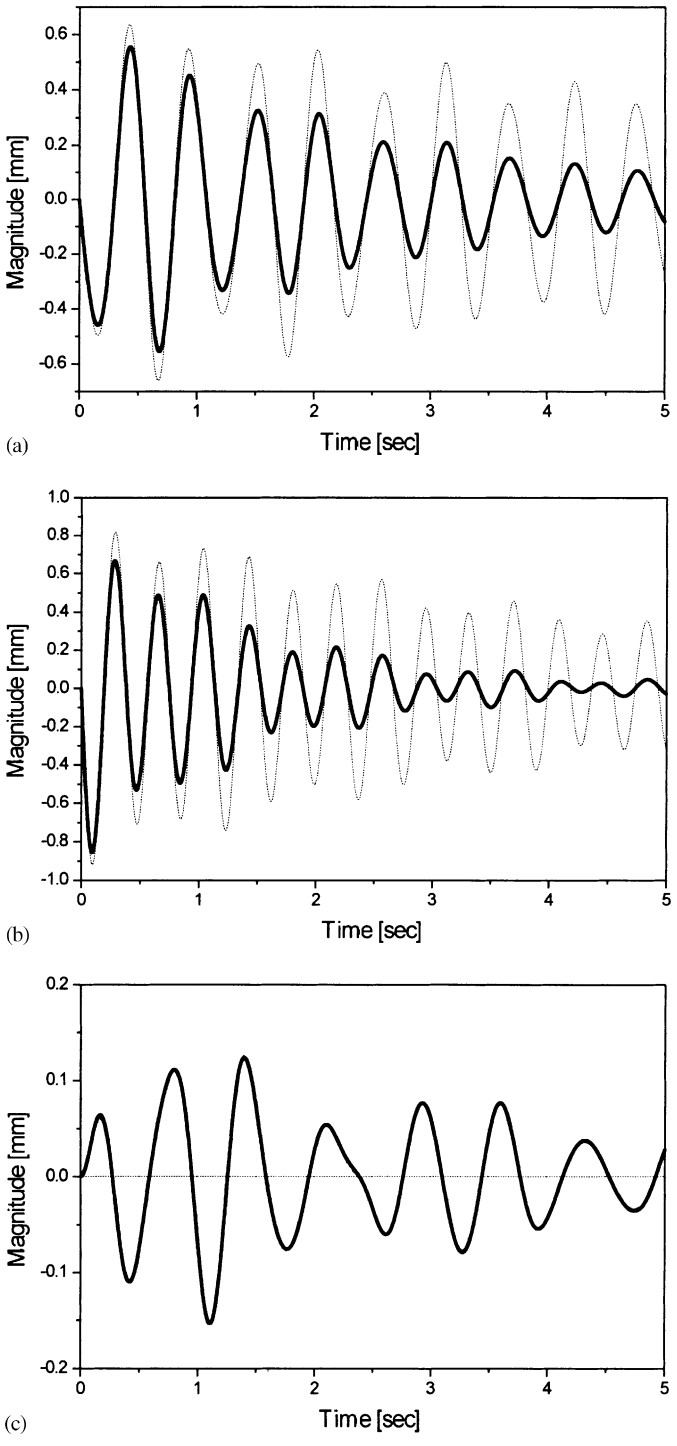

Fig. 6. Responses of the suspension system to the impulse disturbances at points 1 and 4. (a) Bounce-dominant motion, $u_1(t)$, (b) pitch-dominant motion, $u_2(t)$, and (c) roll motion, $u_3(t)$: ……, original system; —– –, passive control system; —— sky-hook control system ($\rho_1 = \rho_2 = \rho_3 = 0.69$); ——, proposed on–off control system ($\rho_1 = 0.66$, $\rho_2 = 0.81$, $\rho_3 = 0$).

Under the pitch and bounce dominant input case (38b), contrary to the previous case, the roll motion, u_3, is not excited because of the input disturbance characteristics for the original system. Now, in order to demonstrate the effect of the target vector specification, we assume $\hat{\boldsymbol{\varphi}}_B \equiv \{0.69 \quad 0.72 \quad 0\}^{\mathrm{T}}$ (marked '$\mathrm{T_B}$' in Fig. 2) considering the pitch and bounce dominant nature of the input disturbances. The optimization (24) gives: $\boldsymbol{\rho}_B = \{0.66\ 0.81\ 0\}^{\mathrm{T}}$, $\lambda_{B+} = 1.40$ and $\boldsymbol{\varphi}_{B+} = \{-0.68\ -0.71\ 0.17\}^{\mathrm{T}}$ (marked '$\mathrm{P_B}$' in Fig. 2) giving the measure of alignment of 0.98. Fig. 6 shows the impulse responses associated with the three components u_i, $i = 1, 2, 3$, of $\mathbf{q}$. Responses of the passive, the sky-hook damper control and the proposed on–off control systems are not distinguable because the proposed control behaves much like the sky-hook damper control as shown in Fig. 7. Note that, in this case, $\ell_s = 0.81$, which is still close to 1, confirming the previous discussions. In this example, because the four identical passive mounts are used in the original system, it is proportionally damped. The eigenvectors of the passive damping matrix $\mathbf{C}$ are identical to the modes of the system. The roll mode is decoupled and is not excited under the latter input case (38b) as seen in Fig. 6(c). But, as a result of the addition of the passive or the semi-active mount at point 1, the system becomes non-proportionally damped and the three modes of the system are coupled with one another. Then, the roll motion is excited under the latter input case (38b) as seen in Fig. 6(c).

Note that the bounce and pitch dominant motions, u_1, and u_2 can be well damped by the passive and the sky-hook damper control systems. Thus, for the target vector composed of u_1 and u_2, it is sufficient to use the passive and the sky-hook damper control systems. However, for the target vector composed mostly of u_3, use of the proposed on–off control is highly recommended.

Now, in order to simulate the excavator cabin suspension system with one semi-active and three passive mounts, which are fixed on the rigid base (vehicle), it is assumed that the base is exposed to

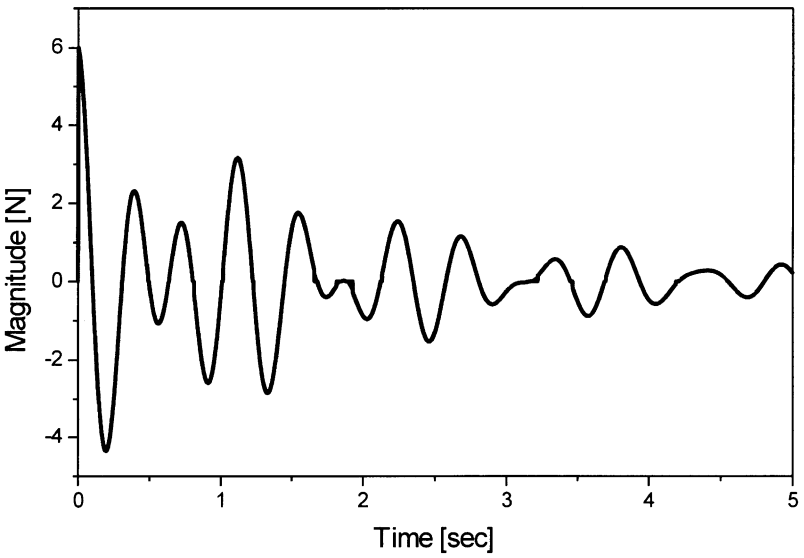

Fig. 7. Control forces to the impulse disturbances at points 1 and 4: ——, sky-hook control system ($\rho_1 = \rho_2 = \rho_3 = 0.69$); ——, proposed on–off control system.

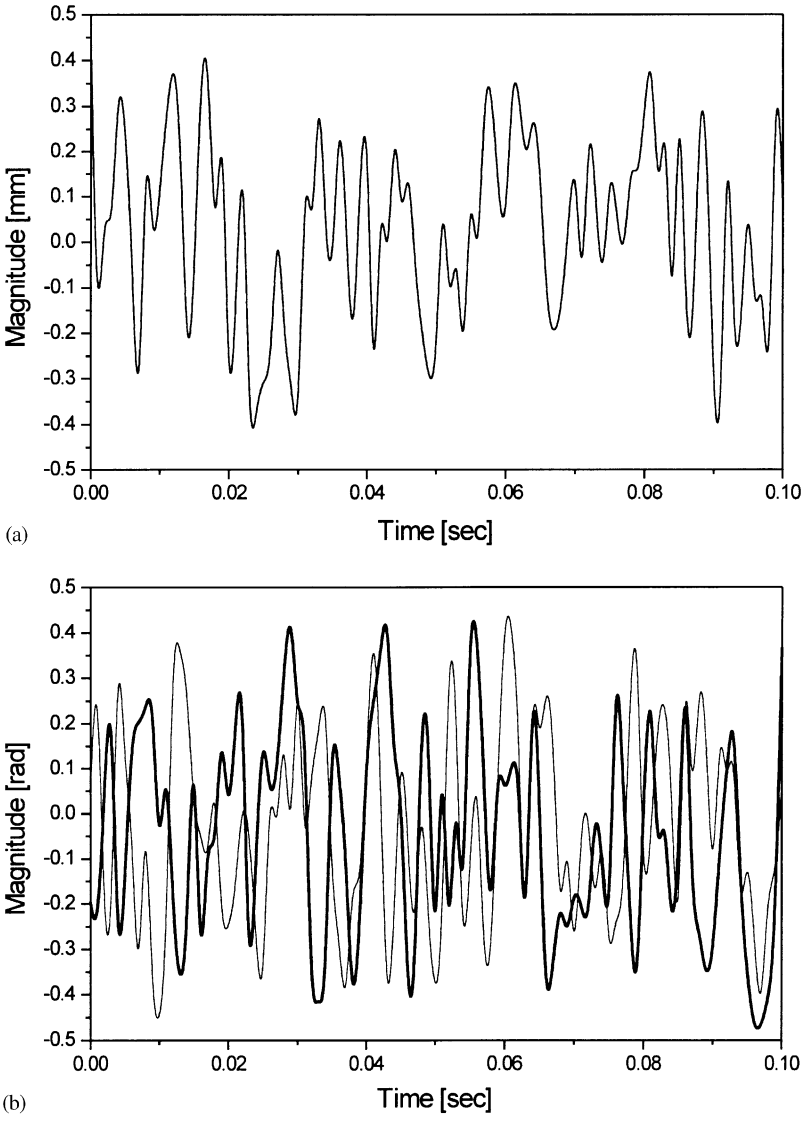

Fig. 8. Random disturbances to the base: (a) bounce, ——, proposed on-off control system (b) pitch and roll disturbances; ——, pitch and ——, roll.

random disturbances. Then, the external disturbances to the cabin suspension system, y_j, $j = 1, 2, 3, 4$, can be represented as

$$\begin{aligned} y_1 &= \tilde{z} + l_2 \sin\tilde{\theta}_y - w_2 \sin\tilde{\theta}_x, \\ y_2 &= \tilde{z} - l_1 \sin\tilde{\theta}_y - w_2 \sin\tilde{\theta}_x, \\ y_3 &= \tilde{z} - l_1 \sin\tilde{\theta}_y + w_1 \sin\tilde{\theta}_x, \\ y_4 &= \tilde{z} + l_2 \sin\tilde{\theta}_y + w_1 \sin\tilde{\theta}_x, \end{aligned} \tag{39}$$

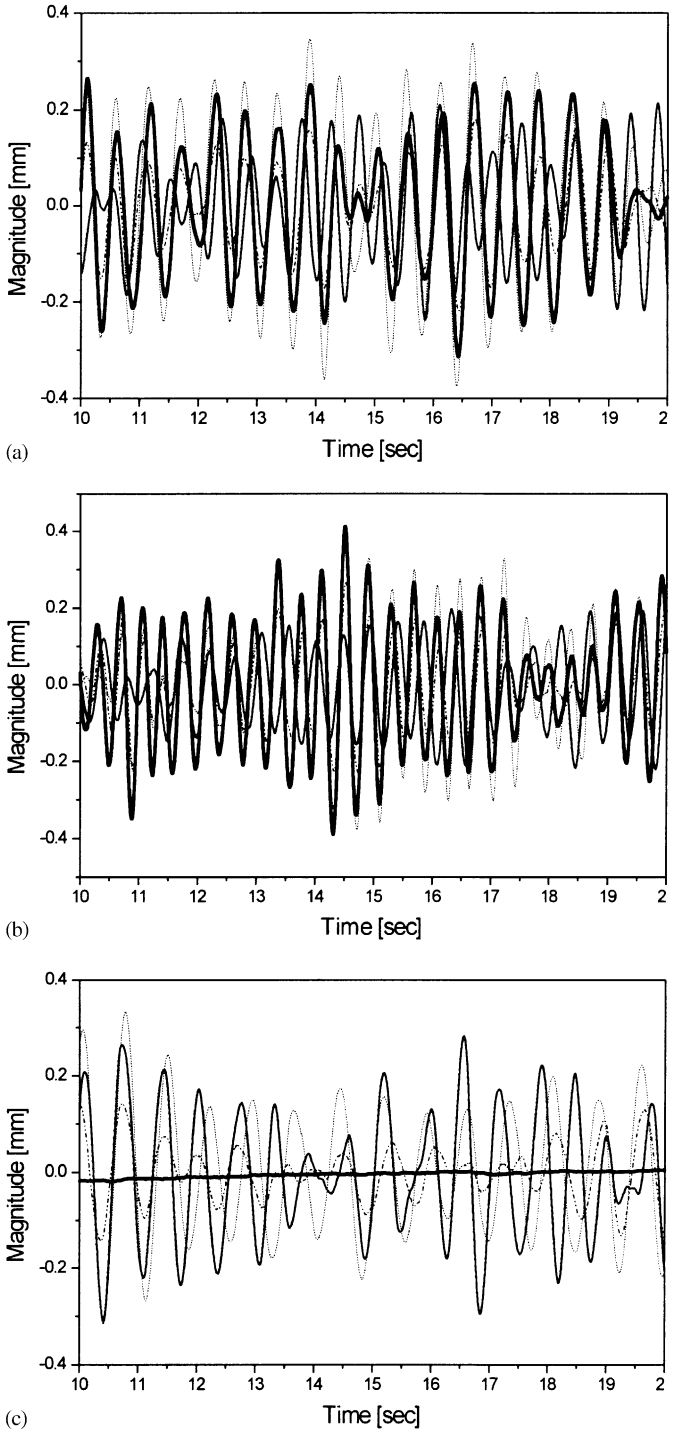

Fig. 9. Responses of the suspension system to the random disturbances at the base. (a) Bounce-dominant motion, $u_1(t)$, (b) pitch-dominant motion, $u_2(t)$, and (c) roll motion, $u_3(t)$: ……, original system; ——, passive control system; ——, sky-hook control system ($\rho_1 = \rho_2 = \rho_3 = 0.69$); ——, proposed on–off control system.

where $\tilde{z}$, $\tilde{\theta}_y$ and $\tilde{\theta}_x$ are the random bounce, pitch and roll motions experienced by the base, as shown in Fig. 8. The random motions of the base have been generated from three independent band-limited white noises with bandwidth of about 500 Hz. Fig. 9 shows the components, u_i, $i = 1, 2, 3$, of the response, $\mathbf{q}$, of the suspension system, when the target vector $\hat{\boldsymbol{\varphi}}_A$ is given as in Eq. (35). Note that, due to the nature of the selected target vector $\hat{\boldsymbol{\varphi}}_A$, the proposed on–off control system gives much smaller (a little larger) values of u_3 (u_1 and u_2) than the passive and the sky-hook damper control systems, similar to the obsevations made with the case of the roll and bounce dominant impulse inputs.

7. Conclusion

Using Lagrange's equations and Lyapunov's direct method, an efficient semi-active on–off damping control law for vibration attenuation of a multi-degree-of-freedom vibratory system has been developed. It minimizes the total vibratory energy of the structure, including the work done by external disturbances, whereas the dissipative energy of the semi-active control device is transformed into the weighted quadratic form and is maximized for the specified vibrational response of the system by a proper assignment of the weighting factors. The vibrational response vector of interest, namely the target mode, is determined at will, considering the vibrational chracteristics of the system and the user's subjective requirement on the performance. Features of the proposed scheme are: it is robust to the system parameters as well as the dynamics of semi-active control devices; it needs theoretically a single semi-active control device; and it needs only the velocity feedback when the system is linearized. A numerical example is treated to demonstrate the application of the proposed control algorithm to a three-degree-of-freedom cabin suspension system with a semi-active mount.

Acknowledgements

The authors are grateful to the Korea Science and Engineering Foundation (KOSEF) for financial support under Contract 97-0102-03-01-3, and Daewoo Heavy Industries & Machinery Ltd. for their assistance in preparing this article.

Appendix A. Derivation of eigensolution of matrix D

Let us define a real symmetric matrix $\mathbf{A}$, which is a general form of the matrix $\mathbf{D}$, as

$$\mathbf{A} = \begin{bmatrix} a_1^2\rho_1 & a_1a_2\dfrac{\rho_1+\rho_2}{2} & \cdots & a_1a_n\dfrac{\rho_1+\rho_n}{2} \\ a_1a_2\dfrac{\rho_1+\rho_2}{2} & a_2^2\rho_2 & \cdots & a_2a_n\dfrac{\rho_2+\rho_n}{2} \\ \vdots & \vdots & \ddots & \vdots \\ a_1a_n\dfrac{\rho_1+\rho_n}{2} & a_2a_n\dfrac{\rho_2+\rho_n}{2} & \cdots & a_n^2\rho_n \end{bmatrix} = \tfrac{1}{2}(\mathbf{P}+\mathbf{P}^{\mathrm{T}}), \tag{A.1}$$

where

$$\mathbf{P} = \begin{pmatrix} a_1^2\rho_1 & a_1a_2\rho_1 & \cdots & a_1a_n\rho_1 \\ a_1a_2\rho_2 & a_2^2\rho_2 & \cdots & a_2a_n\rho_2 \\ \vdots & \vdots & \ddots & \vdots \\ a_1a_n\rho_n & a_2a_n\rho_n & \cdots & a_n^2\rho_n \end{pmatrix} = \mathbf{v}_1\mathbf{v}_2^{\mathrm{T}} \quad \text{and} \quad \mathbf{v}_1 = \begin{Bmatrix} a_1\rho_1 \\ a_2\rho_2 \\ \vdots \\ a_n\rho_n \end{Bmatrix}, \quad \mathbf{v}_2 = \begin{Bmatrix} a_1 \\ a_2 \\ \vdots \\ a_n \end{Bmatrix}.$$

Since *rank* $(\mathbf{p}) \leqslant 1$ and thus *rank* $(\mathbf{A}) \leqslant 2$, there exist a non-zero eigenvalue of $\mathbf{P}$ and one or two non-zero eigenvalues of $\mathbf{A}$. Note here that it holds

$$\mathbf{P}\mathbf{v}_1 = \left(\sum_{i=1}^{n} a_i^2\rho_i\right)\mathbf{v}_1 \tag{A.2}$$

and

$$\mathbf{P}^{\mathrm{T}}\mathbf{v}_2 = \left(\sum_{i=1}^{n} a_i^2\rho_i\right)\mathbf{v}_2. \tag{A.3}$$

For $\mathbf{v} = \mu\mathbf{v}_1 + \mathbf{v}_2$ with an arbitrary constant μ, we obtain

$$\mathbf{A}\mathbf{v} = \frac{1}{2}\left(\left(\sum_{i=1}^{n} a_i^2\rho_i\right)\mathbf{v} + \mu\left(\frac{\sum_{i=1}^{n} a_i^2}{\mu}\mathbf{v}_1 + \mathbf{v}_2\right)\right). \tag{A.4}$$

where $\sum_{i=1}^{n}(a_i\rho_i)^2 = 1$. For the special case when

$$\mu = \frac{\sum_{i=1}^{n} a_i^2}{\mu} \text{ or } \mu = \pm\sqrt{\sum_{i=1}^{n} a_i^2}, \tag{A.5}$$

Eq. (A.4) can be rewritten as

$$\mathbf{A}\mathbf{v} = \frac{1}{2}\left(\sum_{i=1}^{n} a_i^2\rho_i \pm \sqrt{\sum_{i=1}^{n} a_i^2}\right)\mathbf{v}. \tag{A.6}$$

So, the non-zero eigenvalues of $\mathbf{A}$ and the corresponding normalized eigenvectors become

$$\frac{1}{2}\left(\sum_{i=1}^{n} a_i^2\rho_i \pm \sqrt{\sum_{i=1}^{n} a_i^2}\right) \tag{A.7}$$

and

$$\mathbf{v} = \frac{\left\{a_1\left(1 \pm \rho_1\sqrt{\sum_{i=1}^{n} a_i^2}\right) \quad a_2\left(1 \pm \rho_2\sqrt{\sum_{i=1}^{n} a_i^2}\right) \quad \cdots \quad a_n\left(1 \pm \rho_n\sqrt{\sum_{i=1}^{n} a_i^2}\right)\right\}^{\mathrm{T}}}{\sqrt{\sum_{j=1}^{n} a_j\left(1 \pm \rho_j\sqrt{\sum_{i=1}^{n} a_i^2}\right)}}, \tag{A.8}$$

where $\sum_{i=1}^{n}(a_i\rho_i)^2 = 1$.

References

[1] J.H. Kim, C.W. Lee, Y.J. Park, Feedback mode normalization of non-proportionally damped systems for sky-hook damper control design, Proceedings of Asia–Pacific Vibration Conference (A-PVC'99), Singapore, Vol. I, 1999, pp. 547–552.
[2] D.C. Karnopp, M.J. Crosby, R.A. Harwood, Vibration control using semi-active force generators, Journal of Engineering for Industry 96 (1974) 619–626.
[3] G. Leitmann, Semi-active control for vibration attenuation, Journal of Intelligent Material Systems and Structures 5 (1994) 841–846.
[4] G. Leitmann, E. Reithmeier, A control scheme based on ER-material for vibration attenuation of dynamical systems, Applied Mathematics and Computation 70 (1995) 247–259.
[5] N.H. McClamroch, H.P. Garvin, Closed loop structural control using electrorheological dampers, Proceedings of American Control Conference, American Automatic Control Council, (1995) pp. 4173–4177.
[6] L.M. Jansen, S.J. Dyke, Semi-active control strategies for MR dampers: comparative study, Journal of Engineering Mechanics, American Society of Civil Engineers 126 (2000) 795–803.
[7] L. Meirovitch, Methods of Analytical Dynamics, McGraw-Hill, New York, 1970.
[8] M.D. Symans, M.C. Constantinou, Semiactive control systems for seismic protection of structures: a state-of-the-art review, Engineering Structures 21 (1999) 469–487.
[9] J.-J.E. Slotine, Applied Nonlinear Control, Prentice-Hall, Englewood Cliffs, NJ, 1991.
[10] J.P. Keener, Principles of Applied Mathematics: Transformation and Approximation, Addison-Wesley, New York, 1988.